Journal of the American Heart Association

ORIGINAL RESEARCH

Altered Cerebral Microstructure in Adults With Atrial Septal Defect and Ventricular Septal Defect Repaired in Childhood

Benjamin Asschenfeldt, MD, PhD; Lars Evald, MSc, PhD; Camilla Salvig, MD; Johan Heiberg, MD, PhD, DMSc; Leif Østergaard, MD, PhD; Simon Fristed Eskildsen, MSc, PhD; Vibeke Elisabeth Hjortdal, MD, PhD, DMSc

BACKGROUND: Delayed brain development, brain injury, and neurodevelopmental disabilities are commonly observed in infants operated for complex congenital heart defect. Our previous findings of poorer neurodevelopmental outcomes in individuals operated for simple congenital heart defects calls for further etiological clarification. Hence, we examined the microstructural tissue composition in cerebral cortex and subcortical structures in comparison to healthy controls and whether differences were associated with neurodevelopmental outcomes.

METHODS AND RESULTS: Adults (n=62) who underwent surgical closure of an atrial septal defect (n=33) or a ventricular septal defect (n=29) in childhood and a group of healthy, matched controls (n=38) were enrolled. Brain diffusional kurtosis imaging and neuropsychological assessment were performed. Cortical and subcortical tissue microstructure were assessed using mean kurtosis tensor and mean diffusivity and compared between groups and tested for associations with neuropsychological outcomes. Alterations in microstructural tissue composition were found in the parietal, temporal, and occipital lobes in the congenital heart defects, with distinct mean kurtosis tensor cluster-specific changes in the right visual cortex (pericalcarine gyrus, P=0.002; occipital part of fusiform and lingual gyri, P=0.019). Altered microstructural tissue composition in the subcortical structures was uncovered in atrial septal defects but not in ventricular septal defects. Associations were found between altered cerebral microstructure and social recognition and executive function.

CONCLUSIONS: Children operated for simple congenital heart defects demonstrated altered microstructural tissue composition in the cerebral cortex and subcortical structures during adulthood when compared with healthy peers. Alterations in cerebral microstructural tissue composition were associated with poorer neuropsychological performance.

REGISTRATION: URL: https://www.clinicaltrials.gov; Unique identifier: NCT03871881.

Key Words: atrial septal defect ■ cerebral cortex ■ diffusional kurtosis imaging ■ magnetic resonance imaging ■ neurodevelopmental outcome ■ subcortical structures ■ ventricular septal defect

Neurodevelopmental disabilities are frequently described in the population with congenital heart defects (CHD). The disabilities manifest during childhood[1,2] and persist into adolescence[3] indicating a lifelong challenge. The etiology of neurodevelopmental disabilities in CHD is not completely understood, but a key aspect may be the abnormal brain development observed in infants operated for complex CHD.[4–7] Of particular concern are reports of abnormal third trimester deceleration in intrauterine brain growth[6] and a pattern of preoperative brain injury similar to that found in preterm neonates,[4] which suggest an in-utero brain vulnerability in infants with CHDs.

The prenatal factors may indeed be related to brain abnormalities such as reduced brain volumes[8,9] and white matter (WM) alterations[10,11] described in adolescence with complex CHD. Specifically, alterations in WM microstructure and network topology have been

Correspondence to: Benjamin Asschenfeldt, MD, PhD, Department of Cardiothoracic Surgery, Aarhus University Hospital, Palle Juul-Jensens Boulevard 99, 8200 Aarhus N, Denmark. Email: ba@clin.au.dk

For Sources of Funding and Disclosures, see page 15.

JAHA is available at: www.ahajournals.org/journal/jaha

CLINICAL PERSPECTIVE

What Is New?

- The present study demonstrated altered microstructural tissue composition in the cerebral cortex and subcortical structures in a cohort of adults with surgically corrected simple congenital heart defects.
- Changes in cerebral cortical and subcortical microstructural tissue composition were associated with poorer neuropsychological performance.
- Adults with surgically corrected simple congenital heart defects are at risk of an impaired long-term cerebral development.

What Are the Clinical Implications?

- These findings point toward an overlooked early cerebral vulnerability in children with surgically corrected simple congenital heart defects.
- We emphasize the importance of neurodevelopmental surveillance in patients with simple congenital heart defect.

Nonstandard Abbreviations and Acronyms

CHD	congenital heart defect
DKI	diffusional kurtosis imaging
FWE	family-wise error
GM	gray matter
MD	mean diffusivity
MKT	mean kurtosis tensor
WM	white matter

found associated with neurodevelopmental disabilities and clinical risk factors.[10–15] Despite the importance of gray matter (GM) integrity in relation to neurocognitive abilities and motor skills, studies on the long-term impact of CHD on microstructural GM development are lacking, probably due to methodological restrictions.

With the continues technological improvement of MRI, the recently developed method of Diffusional kurtosis imaging (DKI), has shown able to characterize and measure age-related diffusion changes in the developing and aging brain.[16] DKI measures the mean kurtosis tensor (MKT) that is a principal metric of diffusional non-Gaussianity and is believed to arise from diffusion barriers, such as cell membranes and organelles, and water compartments in the tissue.[17,18] Hence, the MKT can be regarded as an index of tissue microstructural complexity.[19–21] The MKT differs from the conventional mean diffusivity (MD) measured with diffusion tensor imaging in that it does not require spatially oriented tissue microstructure and hence is equally applicable on both GM and WM brain tissue and more sensitive to developmental changes.[22]

At present, DKI is primarily considered a research tool when applied on the brain tissue as normal values have not yet been fully established. Nevertheless, the method appears ideal for investigating microstructural gray matter tissue during development.[16]

Considering the simple CHDs, such as atrial septal defect (ASD) and ventricular septal defect (VSD), little is known about their long-term cerebral development. Our group, however, previously reported neurocognitive deficits, similar to those demonstrated in complex CHD, in adults who underwent childhood surgery for a simple CHD.[23] These unsettling findings justify an in-depth investigation of the cerebral development in simple CHD. Accordingly, we now report cortical and subcortical GM microstructural tissue composition measured by DKI in the same group of adults who underwent childhood surgery for a simple CHD compared with healthy peers. Further, we explored associations between neurocognitive deficits and GM microstructural diffusion properties within the group with simple CHD.

METHODS

Design and Study Population

The study was approved by the Regional Committee on Biomedical Research Ethics of the Central Denmark Region (chart: 1-10-72-233-17) and the Danish Data Protection Agency (chart: 2012-58-006). Further, it complies with the World Medical Association's Declaration of Helsinki. In compliance with Danish law, all participants provided written informed consent before enrollment.

This study elaborates on our previously reported neuropsychological status in simple CHD[23] and is registered on clinicaltrials.gov (identifier: NCT03871881). The data that support the findings of this study are available from the corresponding author upon reasonable request.

All participants underwent magnetic resonance imaging (MRI) of the brain and a standardized neuropsychological assessment during the study period from March 2018 to November 2018. Inclusion criteria were (1) surgical closure of isolated ASD or (2) surgical closure of isolated VSD between 1990 and 2000. Exclusion criteria were (1) coexistence of other congenital cardiac or extracardiac abnormalities, (2) syndromes associated with CHD (eg, Down's and 22q11 deletion syndrome), (3) medical history with brain disorder, (4) pregnancy, (5) MRI contraindications, and (6) lack of Danish languages skills. Surgical treatment was performed at Aarhus University Hospital and is

described elsewhere.[23] A group of healthy volunteers, without history of cardiac disease, was included as control group. They were approached through local flyers and internet-based announcements and matched to patients on age, sex, and educational attainment.

MRI Acquisition and Processing

Data Acquisition

Brain MRI was performed using a Siemens Magnetom Prisma 3T MRI system with a 32-channel head coil. Diffusional kurtosis imaging was acquired with both anterior-posterior and posterior-anterior phase encoding directions at b-values 0, 700, 1200, and 2800 s/mm^2. For each phase encoding direction, a total of 191 image volumes were acquired (distribution over b-values: 11/30/60/90; b0 images interleaved throughout the sequence) with repetition time=2972 ms, echo time=65 ms, at istotropic 1.8 mm resolution (acquisition matrix: 112×112, 60 axial slices). A structural T1-weigthed scan was obtained with a Magnetization-Prepared 2 Rapid Acquisition Gradient Echo (MP2RAGE) sequence with the following parameters: repetition time=6.5s, inversion time 1=0.5s, inversion time 2=2.9s, α1=4°, α2=7°, 3D sequence imaged at isotropic 0.9 mm resolution (acquisition matrix: 240×256, 192 sagittal slices) with turbo factor of 144 as defined by others.[24]

MRI Analyses

MP2RAGE images were processed using the framework described in Aubert-Broche et al[25] Images were denoised, bias field corrected, and linear and nonlinear registered to Montreal Neurological Institute space. Images were then skull-stripped and classified into GM, WM, and cerebrospinal fluid . Subcortical nuclei were either segmented using a patch-based estimator (hippocampus and thalamus)[26] or by merging tissue classes with an atlas in Montreal Neurological Institute space (caudate, fornix, putamen, and globus pallidus). For each hemisphere of the cerebrum, surfaces in 3D were fitted to the WM, midcortical layer, and pial surface using fast accurate cortex extraction.[27]

The DKI images were denoised[28] and corrected for artifacts related to Gibbs ringing,[29] motion and eddy currents.[30] MD and MKT were calculated using an in-house pipeline based on Hansen et al[31] b0 images were coregistered[32] to MP2RAGE images and cortical surfaces were transformed to DKI native space. DKI parameters were interpolated and mapped to the midcortical surface thereby minimizing partial volume effects. Individual surfaces were registered[33] to an average nonlinear template surface in Montreal Neurological Institute space.[34] DKI parameters were then mapped to the average template and smoothed using a geodesic smoothing kernel with a full width half max of 20 mm. The segmentations of subcortical nuclei were transformed to native DKI space and the mean of each DKI parameter was calculated for each nucleus.

Neurodevelopmental Assessment

The neurodevelopmental assessment included the Wechsler Adult Intelligence Scale – Fourth Edition,[35] the Delis-Kaplan Executive Function System,[36] the Rey-Osterreith Complex Figure Test,[37–39] the Rey Auditory Verbal Learning Test,[40] the Reading the Mind in the Eyes Test[41] and was previously published.[23]

Statistical Analysis

Data are presented as mean±SD, absolute numbers with percentages of participants, or as medians with total ranges, as appropriate. Continuous data were compared using Student unpaired *t* tests, Wilcoxon rank-sum tests, or multivariable linear regression adjusted for sex and age, as appropriate. Binary data are presented as absolute numbers and relative percentages and compared using the χ^2 tests. Statistical significance was considered as *P* value <0.05. Multiple testing was accounted for by calculating a false discovery rate q-value.[42] Cortical parameter maps were fitted with a general linear model with age and sex as fixed effects for each DKI parameter and cortical thickness using the SurfStat toolbox[43] running in MATLAB 2016b (MathWorks, Natick, MA). The statistical maps were family-wise error (FWE) corrected using a cluster defining threshold of α=0.001.[44] Associations between MRI variables and neuropsychological outcomes were examined using multivariable linear regression adjusted for age and sex. All statistical analyses, except the statistical maps, were conducted using Stata/SE 15.1 for Mac (StataCorp, College Station, TX).

Sample Size Justification

A sample size justification with a power of 80% and a significance level of 0.05 using the Student *t* test for this cohort of participants has been published elsewhere.[23]

RESULTS

Cohort

A total of 66 subjects with CHDs and 40 controls were enrolled in the study. MRI data from 6 subjects were excluded from further analyses because of claustrophobia/anxiety during MRI or inadequate image quality. Hence, 62 CHD participants (ASD=33 and VSD=29) and 38 controls were included in the MRI analyses. At enrollment, the mean age was 24.5±5.1 years in the group with CHDs and 25.6±4.5 years in the control group (*P*=0.925), and sex was evenly distributed between groups. Information on basic demographics, educational

achievement, perioperative information, and medical history of the study participants are reported elsewere.[23]

Group Differences of Diffusional Variables Between CHD and Control Subjects

Cortical Gray Matter Microstructure

Comparison of MKT and MD between the CHD and control participants are shown in Figures 1 and 2, respectively. We identified substantial differences in the cortical GM microstructural tissue composition in the group with CHDs when compared with the control group. The group with CHDs had higher MKT located in the occipital (medial occipital surface), parietal (precuneus and cuneus domains), and temporal (the inferior temporal gyri) lobes. A higher cluster-specific MKT value in the right pericalcarine gyrus and in the occipital part of the fusiform and lingual gyri remained after FWE correction (P=0.002 and 0.019, respectively).

A subgroup analysis showed that primarily the group with ASDs contributed to the higher MKT in the pericalcarine gyrus and, moreover, had a higher MKT value in the right parietal lobe at the temporoparietal junction that remained significant after FWE correction (P=0.005 and 0.025, respectively). The group with VSDs had a higher MKT value in the fusiform and lingual gyri compared with the control group; however, significance did not remain after FWE-correction. Moreover, the group with VSDs disclosed a higher MD in the cuneus and precuneus domains compared with controls. Higher MD values of the right parieto-occipital fissure remained significant after FWE correction (P=0.039).

Subcortical GM Microstructure

The MKT and MD values of subcortical structures in the CHD participants compared with that in control participants are shown in Table 1 and 2, respectively. The group with CHDs disclosed subtle changes in DKI parameters (lower MKT in the left fornix, P=0.037); however, a subgroup analysis revealed various MKT and MD differences in the left and right hemisphere subcortical structures in the group with ASDs (left caudate nucleus, P=0.048; left fornix, P=0.021; right thalamus, P=0.028) compared with controls. Subcortical MKT and MD values in the group with VSDs were not different from those in the control group.

Correlates of Neurodevelopmental Outcomes

Cortical GM Microstructure

Neurodevelopmental outcomes were examined for associations with cortical surface DKI parameters. First, we tested for general associations between neuropsychological outcomes and whole cortical surface DKI parameters (Figure 3 through 6). This revealed several significant associations between cortical surface DKI parameters and the neuropsychological abilities of social recognition (Figure 3) and executive functions (Figure 4 through 6), which all survived FWE correction. These associations are summarized in Table 3. Associations in the group with ASDs were unique as no similar associations were found in the control group; however, the association in the group with VSDs (cortical MKT value and Trail Making Test) was similarly observed in the control group.

Second, we tested for specific associations between neuropsychological outcomes and mean values within FWE-corrected clusters with altered cortical surface DKI parameters. However, only few associations were found, and none remained significant after false discovery rate correction (Table 4).

Subcortical GM Microstructure

Neurodevelopmental outcomes were examined for associations with DKI parameters of the subcortical structures. First, general associations were revealed within the groups; however, these varied from group to group, and none remained significant after false discovery rate -correction. Second, we tested for specific associations between neuropsychological outcomes and subcortical structures with altered DKI parameters. This revealed associations between the basal ganglia (left caudate nucleus) and intelligence and verbal learning and memory, and between the limbic system (left fornix and right thalamus) and executive function (verbal fluency test) in the group with ASDs, which are shown in Table 5. Interestingly, the MKT and MD of the left fornix were strongly associated with executive function (verbal fluency test) and remained significant after false discovery rate correction. No similar associations were found in the control group.

DISCUSSION

Young adults who underwent full-flow bypass surgery for an ASD or VSD during early childhood revealed altered microstructural tissue properties in the cortical GM and in subcortical structures when compared with healthy peers. Key differences in microstructural properties were located in the visual cortex domain in the occipital lobe and in structures of the limbic system and basal ganglia. Associations between altered cerebral microstructural properties and worse neuropsychological outcomes were uncovered in the group with ASDs.

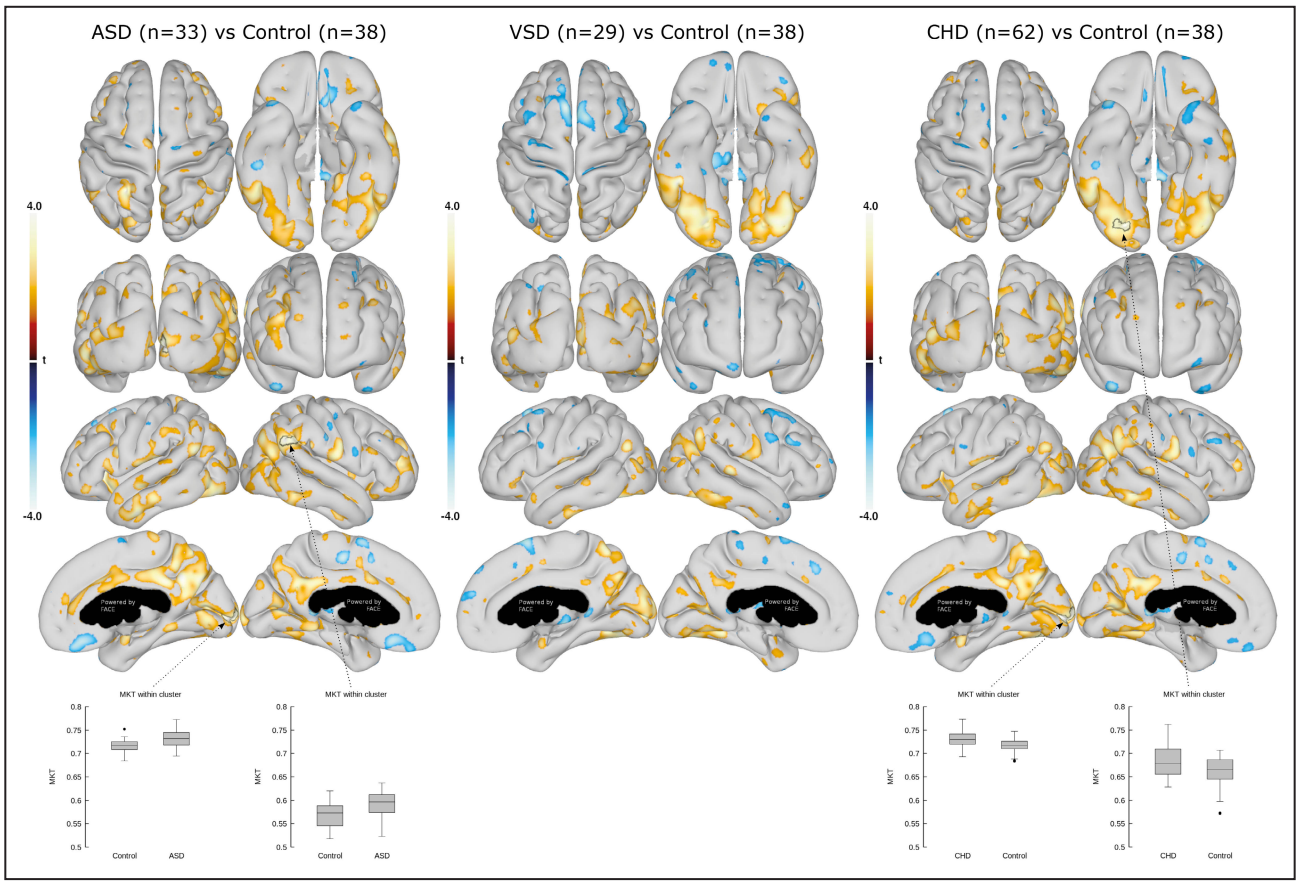

Figure 1. Mean kurtosis tensor (MKT) in the cortical gray matter.
Comparison of cortical GM MKT between ASDs and controls (left), VSDs and controls (middle), and all CHDs and controls (right). Data are presented as statistical t-value maps adjusted for age and sex using linear regression and thresholded at $P<0.05$. Negative t-values indicate reductions (blue nuances), and positive t-values indicate increases (red nuances) in MKT. The black arrows and outlines denote clusters surviving family-wise error correction for multiple comparisons at $\alpha=0.001$. Box plots with group mean and 95% CI are shown for the most significant clusters. ASD indicates atrial septal defect; CHD, congenital heart defect; and VSD, ventricular septal defect.

Altered Cerebral Microstructural Properties

Abnormal Microstructural Properties of the Cerebral Cortex

Applying the DKI technique on this study cohort revealed increased cortical kurtosis and diffusivity in GM of adults who were operated for a simple CHD during childhood. The main alterations in cortical microstructure were located in the occipital region, at the primary and secondary visual cortex in the group with CHDs. MKT was increased in the group with CHDs but more pronounced in the group with ASDs than in the group with VSDs. Moreover, the group with VSDs had increased MD in the right cuneus in the occipital region.

In the context of our findings, the term *microstructure* refers to brain tissue structures that act as barriers for free diffusion of water such as cell membranes, myelin layers, axon sheaths, etc. Also, the term *properties* refer to the tissue characteristics in term of number, density, orientation, and organization of microstructures.

In the healthy brain, increased kurtosis and diffusivity are associated with brain maturation and improved cognitive function[17,45] and a higher complexity of the tissue microstructure.[17,18,46] The higher cortical MKT and MD values in our study may therefore indicate more diffusion barriers, that is, more densely packed cells, higher dendritic density, or higher axonal density.[47] More diffusion barriers affect the motion of water molecules and subsequently the kurtosis and diffusion coefficient. Given that in patients with simple CHD, the MKT relationship in cognitive function appears to follow the same pattern as in healthy individuals (increased kurtosis associated with better cognitive function), we speculate that the observed MKT and MD increase in patients with ASD and VSD may mirror a layered effect of pathology in addition to typical microstructural organization in occipital GM.

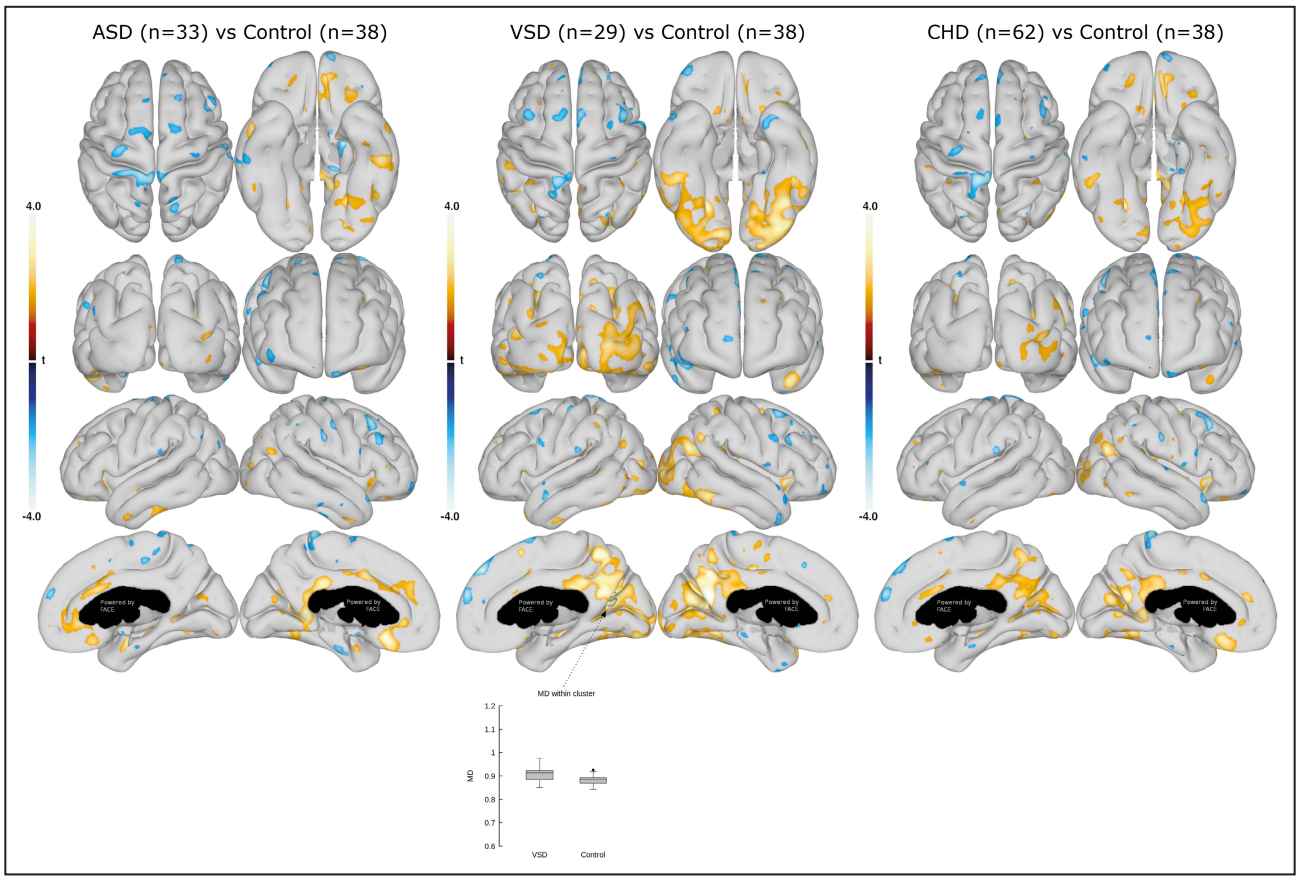

Figure 2. Mean diffusivity (MD) in the cortical gray matter.
Comparison of cortical GM MD between the ASDs and controls (left), VSDs and controls (middle), and all CHDs and controls (right). Data are presented as statistical t-value maps adjusted for age and sex using linear regression and thresholded at $P<0.05$. Negative t-values indicate reductions (blue nuances), and positive t-values indicate increases (red nuances) in MD. The black arrow and outline denote a cluster surviving family-wise error correction for multiple comparisons at $\alpha=0.001$. Box plots with group mean and 95% CI are shown for the most significant clusters. ASD indicates atrial septal defect; CHD, congenital heart defect; and VSD, ventricular septal defect.

Owing to the lack of histological studies on the brain in adults with simple CHD, a thorough explanation to the alterations in cortical microstructure remains speculative. However, alterations in microstructural GM properties have been reported in cohorts with other diseases or conditions, such as attention-deficit hyperactivity disorder, Parkinson's disease, multiple sclerosis, and schizophrenia.[17,45,48–50] Similar to our findings, McKenna et al.[50] demonstrated an increased MKT and MD in cortical GM within several brain lobes in patients with schizophrenia, however, not in the occipital lobe as in our cohort. McKenna et al.[50] speculate whether the microcellular changes were an indicator of one or several pathological mechanisms including higher-order inflammation, protein accumulation, oxidative stress, iron deposits, and hypometabolism pathology. In animal studies, increased MKT has also been associated with increased astrocyte immunoreactivity, fiber dispersion, and protein deposition in mouse neurodegenerative models including brain trauma and Huntington and Alzheimer disorders.[51–53] In all, increased kurtosis and diffusivity values in GM tissue may be associated with pathological changes on a microcellular level.

Abnormal Microstructural Properties of Subcortical Structures

Alterations were located within the limbic system and basal ganglia in the patient group. The term "limbic system" refers to a collection of subcortical structures involved in processing emotion and memory. In the left fornix, a structure within the limbic system, we demonstrated a prominent decrease in MKT and increase in MD in the group with ASDs. The fornix is a WM bundle in the limbic circuits, a predominant outflow tract of the hippocampus and one of the most important subcortical structures related to memory.[54,55] A rapid increase

Table 1. Mean Kurtosis Tensor Values of Subcortical Gray Matter in the Congenital Heart Defect and Control Participants

	ASD (n=33)	VSD (n=29)	CHD (n=62)	Control (n=38)	*P* value, ASD versus control*	*P* value, VSD versus control*	*P* value, CHD versus control*
Left							
Caudate nucleus	0.6794±0.0228	0.6602±0.0250	0.6704±0.0256	0.6672±0.0262	0.048†	0.570	0.454
Putamen	0.7444±0.0347	0.7211±0.0298	0.7335±0.0343	0.7366±0.0305	0.476	0.260	0.686
Globus pallidus	1.0279±0.0617	1.0056±0.0694	1.0175±0.0658	1.0021±0.0407	0.055	0.209	0.181
Subthalamicus nucleus	1.1591±0.0555	1.1615±0.0561	1.1602±0.0553	1.1655±0.0689	0.612	0.727	0.741
Fornix	0.7616±0.0445	0.7666±0.0339	0.7639±0.0397	0.7809±0.0356	0.021†	0.169	0.037†
Hippocampus	0.7193±0.0318	0.7138±0.0263	0.7168±0.0292	0.7122±0.0289	0.200	0.282	0.246
Thalamus	0.8374±0.0361	0.8238±0.0296	0.8311±0.0336	0.8308±0.0324	0.358	0.664	0.754
Right							
Caudate nucleus	0.6763±0.0249	0.6592±0.0205	0.6683±0.0243	0.6706±0.0224	0.446	0.116	0.695
Putamen	0.7383±0.0394	0.7145±0.0315	0.7272±0.0376	0.7296±0.0259	0.422	0.159	0.783
Globus pallidus	1.0159±0.0682	0.9922±0.0607	1.0048±0.0654	0.9960±0.0402	0.153	0.727	0.393
Subthalamicus nucleus	1.1380±0.0454	1.1326±0.0612	1.1355±0.0530	1.1385±0.0539	0.834	0.877	0.781
Fornix	0.7774±0.0434	0.7670±0.0371	0.7725±0.0406	0.7764±0.0326	0.700	0.404	0.663
Hippocampus	0.7150±0.0282	0.7070±0.0234	0.7112±0.0262	0.7091±0.0214	0.292	0.658	0.507
Thalamus	0.8416±0.0358	0.8254±0.0297	0.8340±0.0338	0.8411±0.0322	0.994	0.121	0.338

Data are presented as mean±SD. ASD indicates atrial septal defect; CHD, congenital heart defect; and VSD, ventricular septal defect.
**P* values are determined by multivariable linear regression adjusted for age and sex.
†$P<0.05$.

Table 2. Mean Diffusivity Values of Subcortical Gray Matter for the Congenital Heart Defect and Control Participants

	ASD (n=33)	VSD (n=29)	CHD (n=62)	Control (n=38)	*P* value, ASD versus control*	*P* value, VSD versus control*	*P* value, All CHD versus control*
Left							
Caudate nucleus	1.0100±0.0601	1.0061±0.0520	1.0082±0.0560	1.0266±0.1598	0.914	0.303	0.466
Putamen	0.8067±0.0236	0.8060±0.0249	0.8064±0.0240	0.8078±0.0226	0.696	0.589	0.836
Globus pallidus	0.8565±0.0458	0.8573±0.0436	0.8568±0.0444	0.8619±0.0411	0.840	0.435	0.656
Subthalamicus nucleus	0.8365±0.0531	0.8171±0.0515	0.8274±0.0529	0.8190±0.0629	0.157	0.560	0.459
Fornix	1.5583±0.1719	1.5270±0.1148	1.5436±0.1476	1.4925±0.1334	0.021†	0.277	0.072
Hippocampus	0.9859±0.0401	0.9888±0.0274	0.9872±0.0345	0.9898±0.0332	0.544	0.416	0.791
Thalamus	0.8813±0.0248	0.8810±0.0252	0.8811±0.0248	0.8810±0.0304	0.337	0.798	0.815
Right							
Caudate nucleus	1.0092±0.0520	1.0022±0.0510	1.0059±0.0512	1.0010±0.0631	0.130	0.583	0.571
Putamen	0.8039±0.0191	0.7997±0.0217	0.8019±0.0203	0.7976±0.0213	0.054	0.991	0.272
Globus pallidus	0.8385±0.0404	0.8466±0.0345	0.8423±0.0377	0.8450±0.0403	0.914	0.859	0.820
Subthalamicus nucleus	0.8473±0.0687	0.8403±0.0745	0.8440±0.0710	0.8420±0.0562	0.432	0.819	0.740
Fornix	1.4909±0.1462	1.5170±0.1380	1.5031±0.1419	1.4879±0.1365	0.493	0.499	0.559
Hippocampus	0.9817±0.0375	0.9816±0.0295	0.9817±0.0337	0.9842±0.0305	0.517	0.491	0.742
Thalamus	0.8972±0.0272	0.8955±0.0304	0.8964±0.0285	0.8868±0.0250	0.028†	0.248	0.059

Data are presented as mean±SD. ASD indicates atrial septal defect; CHD, congenital heart defect; and VSD, ventricular septal defect.
**P* values are determined by multivariable linear regression adjusted for age and sex.
†*P*<0.05.

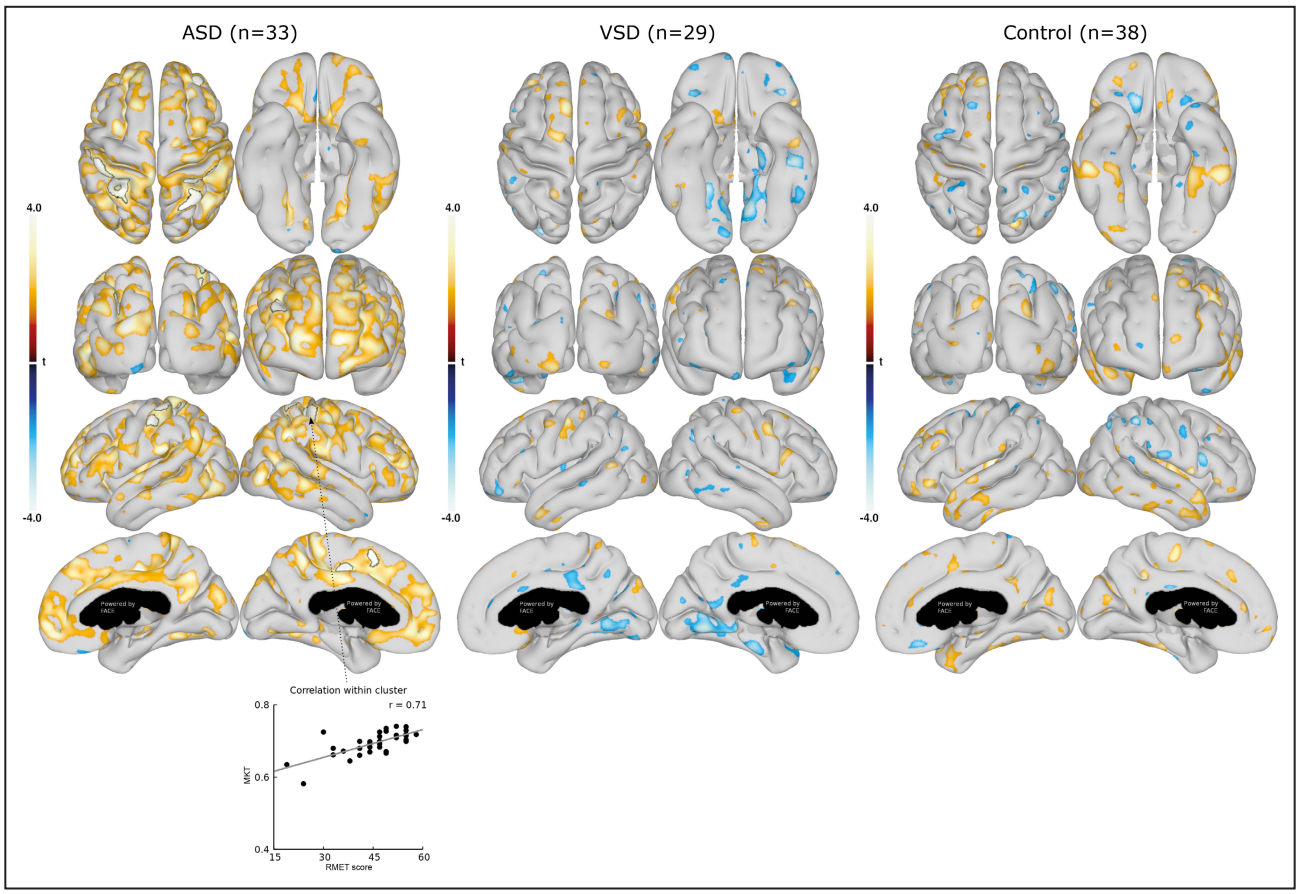

Figure 3. Association between mean kurtosis tensor (MKT) in cortical gray matter and social recognition (Reading the Mind in the Eyes Test).
Associations between cortical gray matter MKT and RMET are shown for the group with ASDs (left), group with VSDs (middle), and control group (right). Data are presented as statistical t-value maps adjusted for age and sex using linear regression and thresholded at $P<0.05$. Negative t-values indicate negative associations (blue nuances), and positive t-values indicate positive associations (red nuances). The black outlines denote clusters surviving family-wise error correction for multiple comparisons at $\alpha=0.001$. A scatterplot, with Pearson's correlation (grey line), shows the association between MKT value and RMET score in the most significant cluster. ASD indicates atrial septal defect; RMET, Reading the Mind in the Eyes Test; and VSD, ventricular septal defect.

in WM MKT normally occurs during the transition from adolescence to adulthood reflecting the late stages of cerebral maturation.[16]

In adulthood, MKT decrease is probably related to the degenerative changes and neuronal shrinkage that occurs with normal aging.[16] It is reasonable to assume that a lower WM MKT during adolescence may result in an abnormal WM MKT in the late decades of life. Therefore, the lower WM MKT of the left fornix in the group with CHDs may imply an increased age-dependent cerebral vulnerability.

Alzheimer's disease causes alterations in the fornix with demyelination or axonal loss compromising the microstructural tissue properties.[56] As a consequence of these pathological changes in the limbic system, impairment in memory and executive function emerge. In view of the Alzheimer's disease pathology, we speculate whether the fornix alterations found in the group with ASDs may predispose to an accelerated decline of memory and executive functions in the late decades of life. This concern is supported by the previously demonstrated increased risk of dementia in adults with CHDs, including acyanotic CHD, compared with the general population.[57] Also, it is worrying that our cohort of adults with CHDs already appear to have widespread impaired neurodevelopmental outcomes including poorer memory and executive functions.[23]

The thalamus, another limbic structure, showed a unilateral increase in MD in the group with ASDs. This is somewhat an interesting finding being mindful of the visual system. The group with ASDs had significant MKT changes in the right primary visual cortex, which receives afferent signals from the corpus geniculatum laterale, an area of thalamus. Therefore, the finding of microstructural changes in both thalamus and the primary visual cortex in the right cerebral hemisphere may indicate abnormalities in the visual system in the group with ASDs.

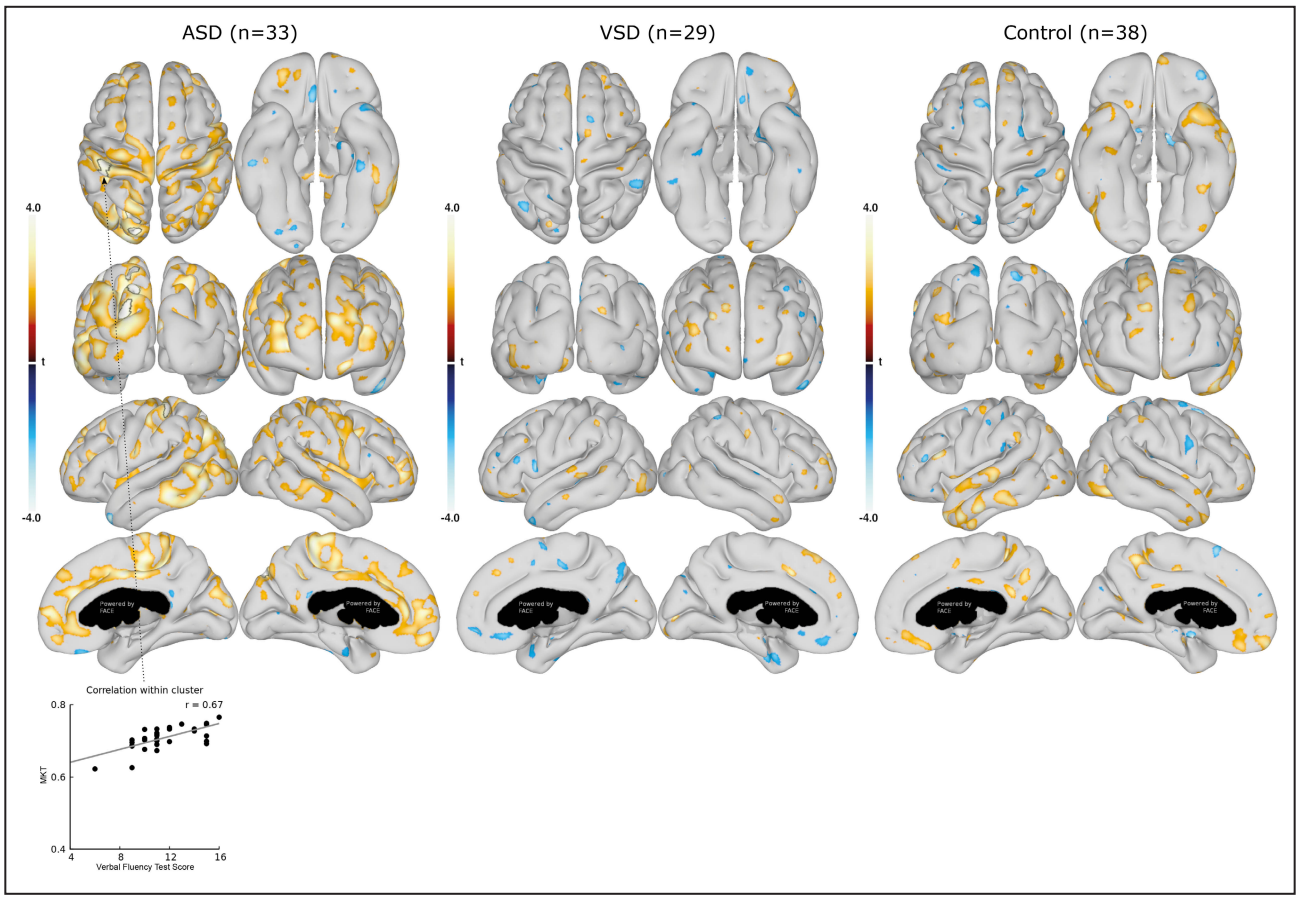

Figure 4. Association between mean kurtosis tensor (MKT) in cortical gray matter and executive function (Verbal Fluency Test).

Associations between the cortical gray matter MKT and the Verbal Fluency Test score are shown for the group with ASDs (left), group with VSDs (middle), and control group (right). Data are presented as statistical t-value maps adjusted for age and sex using linear regression and thresholded at $P<0.05$. Negative t-values indicate negative associations (blue nuances), and positive t-values indicate positive associations (red nuances). The black outlines denote clusters surviving family-wise error correction for multiple comparisons at $\alpha=0.001$. A scatterplot, with Pearson's correlation (grey line), shows the association between MKT values and Verbal Fluency Test score in the most significant cluster. ASD indicates atrial septal defect; and VSD, ventricular septal defect.

The term "basal ganglia" refers to deep subcortical nuclei responsible for primarily motor control and several cognitive functions. Abnormalities within the basal ganglia, are previously demonstrated in patients with dextro-transposition of the great arteries (d-TGA) during adolescence who had reduced volume in the bilateral striatum and pallidum.[58] In accordance, we observed altered microstructural tissue properties in the left caudate nucleus, a part of the striatum, in the group with ASDs compared with controls. Our finding reflects a denser microstructural composition in the caudate nucleus but may still mirror a layered effect of pathology as in the cortical GM.

Differences in Cerebral Microstructure Between the Populations With ASD and VSD

The differences in microstructural cerebral properties between the populations with ASD and VSD need to be interpreted with caution because of the small size of our populations. On the other hand, differences between patients with ASD and VSD in our previous studies may confirm that they truly are different in some aspects.

We know from some of our previous register-based studies that preterm birth is more prevalent in ASD than in VSD,[59] that babies with VSD have smaller head circumferences at birth whereas babies with ASD have head sizes comparable to the background population,[60] and that babies with VSD have a smaller placenta when born.[61] Hence, the differences in the cerebral MKT and MD between ASD and VSD may not be so surprising after all but remains speculative at his point.

Altered Cerebral Morphology in CHD

The microstructural properties of GM are sparsely described in patients with CHDs. Nevertheless, our

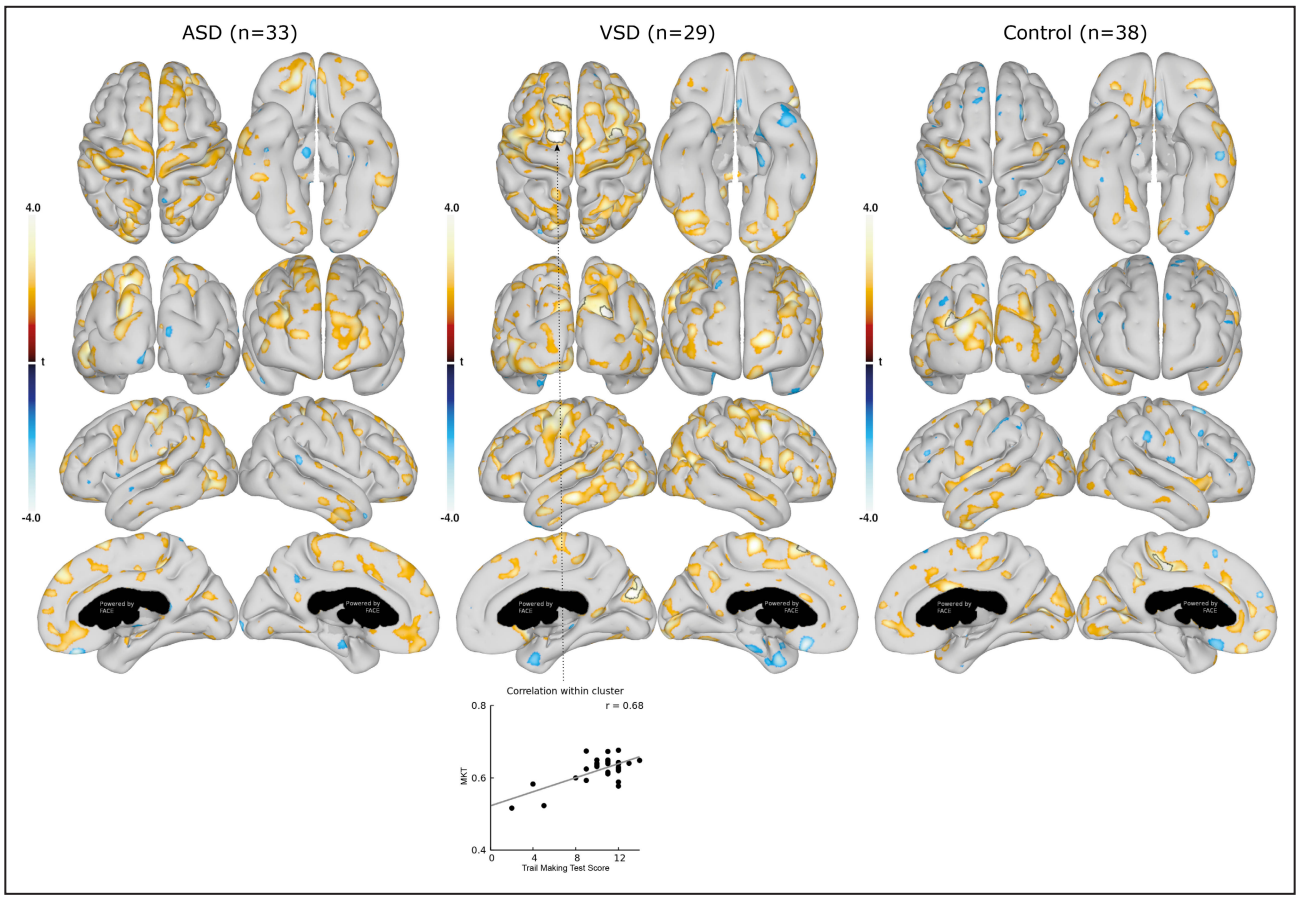

Figure 5. Association between mean kurtosis tensor (MKT) in cortical gray matter and executive function (Delis-Kaplan Executive Function System: Trail Making Test).
Associations between the cortical gray matter MKT and the Trail Making Test scores are shown for the group with ASDs (left), group with VSDs (middle), and control group (right). Data are presented as statistical t-value maps adjusted for age and sex using linear regression and thresholded at $P<0.05$. Negative t-values indicate negative associations (blue nuances), and positive t-values indicate positive associations (red nuances). The black outlines denote clusters surviving family-wise error correction for multiple comparisons at $\alpha=0.001$. A scatterplot, with Pearson's correlation (grey line), shows the association between MKT values and Trail Making Test score in the most significant cluster. ASD indicates atrial septal defect; and VSD, ventricular septal defect.

findings are in agreement with previous studies reporting abnormal cerebral morphology in various cohorts with CHDs during early adulthood. In the study by Watson et al.,[58] a widespread reduced volume of the cortical surface and subcortical brain regions in adolescents with d-TGA were demonstrated. Additionally, Latal et al.[62] found a reduced volume of the limbic structure of hippocampus in a cohort of mixed CHDs, and Von Rhein et al.[9] reported GM abnormalities such as reduced volume of the cortical GM and subcortical structures of the basal ganglia and hippocampus in adolescents with acyanotic CHD.

Although in our previous study we found normal brain volumes in the cohort with simple CHDs,[23] in the present study we established worrying evidence of a compromised cerebral microstructure in patients with simple CHD that is in agreement with the abnormalities in GM morphology previously described by others.[9,58,62]

Neurodevelopmental Outcome and Cerebral Microstructural Properties

We found several associations between neuropsychological outcomes and DKI parameters of the cerebral GM in the cohort with CHDs, albeit not in the control group. In general, associations were more pronounced in the group with ASDs where these were present in both cortical GM and subcortical structures whereas associations in the group with VSDs were present only in the cortical GM. Interestingly, outcomes in social recognition and executive function were highly associated with DKI parameters in both cortical GM and subcortical structures. Associations in social recognition were primarily found in the group with ASDs; however, associations in executive function were present in both the groups with ASDs and VSDs. These associations in our cohort with CHDs point toward an effect

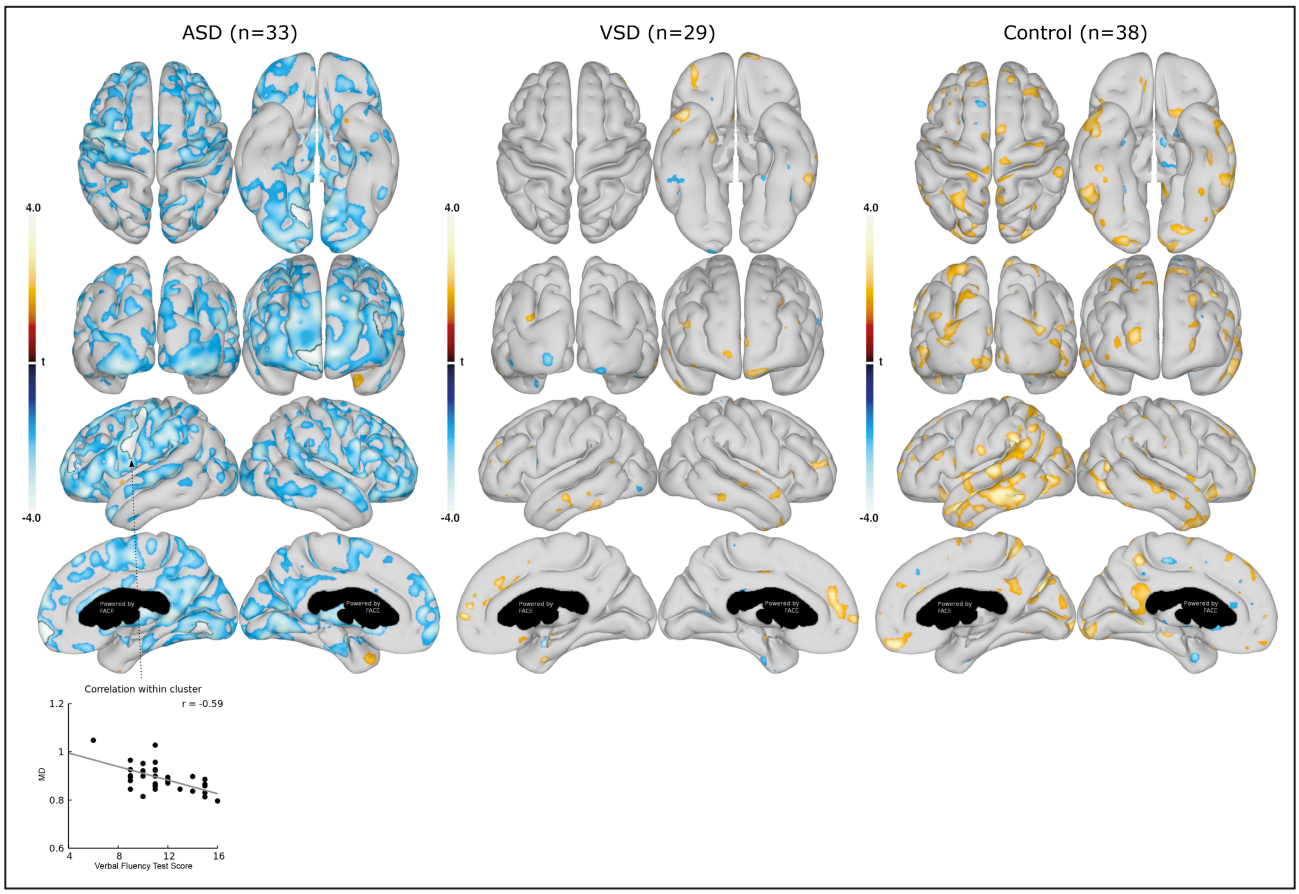

Figure 6. Association between mean diffusivity (MD) in cortical gray matter and executive function (Verbal Fluency Test). Associations between the cortical gray matter MD and the Verbal Fluency Test scores are shown for the group with ASDs (left), group with VSDs (middle), and control group (right). Data are presented as statistical t-value maps adjusted for age and sex using linear regression and thresholded at $P<0.05$. Negative t-values indicate negative associations (blue nuances), and positive t-values indicate positive associations (red nuances). The black outlines denote clusters surviving family-wise error correction for multiple comparisons at $\alpha=0.001$. A scatterplot, with Pearson's correlation (grey line), shows the association between MD values and Verbal Fluency Test score in the most significant cluster. ASD indicates atrial septal defect; and VSD, ventricular septal defect.

of cortical and subcortical microstructural changes on neurodevelopmental outcome.

In adolescents with complex CHD, impairment in social cognition and executive functioning is a well-known problem, which may lead to psychosocial disorders and a lower quality of life.[63] Despite evidence of neurocognitive abnormalities in CHD adolescents, studies combining neurocognitive outcomes and brain MRI diffusion are limited. Rollins et al. reported reduced fractional anisotropy in a subset of WM regions in adolescents with d-TGA, which were associated with poorer cognition including a lower executive function scored by parental questionaires.[10] In an elaborate study on the same cohort with d-TGA, the authors described specific WM tracts that were independently associated with performance on memory and attention tasks.[11]

Associations between neurodevelopmental outcomes and brain abnormalities identified by conventional MRI have also been reported.[64–66] Bellinger et al. showed that focal infarction or cerebral atrophy was associated with poorer outcomes in executive function and social cognition in adolescents who underwent the Fontan procedure.[66] Contrarily, in a similar study but with adolescents with a d-TGA cardiac physiology, no associations were found between brain abnormalities and neurocognitive outcomes.[3] To elucidate the relationship between neurocognitive outcomes and alterations to the microstructural composition of brain tissue in CHDs, studies on larger patient cohorts are warranted, preferably in a longitudinal setup.

Potential Mechanisms

A considerable aspect in our main findings is the occurrence of altered tissue microstructure in posterior areas of the brain (including pericalcarine gyrus, fusiform, and lingual gyri), which are mainly supplied by

Table 3. Summarized Associations Between Neuropsychological Outcomes and Cortical Surface Diffusional Kurtosis Imaging Values for Congenital Heart Defect and Control Participants

Neuropsychological outcome	Cortical diffusional kurtosis imaging values
Atrial septal defect	
Social recognition*	Cortical MKT of bilateral frontal and parietal lobes
Executive function†	Cortical MKT of left parietal and occipital lobes
Executive function†	Cortical mean diffusivity of bilateral frontal and right occipital lobes
Ventricular septal defect	
Executive function‡	Cortical MKT of bilateral frontal and right occipital lobes

MKT indicates mean kurtosis tensor.
*Reading the Mind in the Eyes Test.
†Delis-Kaplan Executive Function System: Verbal Fluency Test.
‡Delis-Kaplan Executive Function System: Trail Making Test.

the posterior cerebral artery. As the posterior cerebral artery departs from the vertebral artery via the basilar artery, one may speculate whether tissue microstructure could also be altered in the cerebellum. Though we did not include cerebellum in our analysis, previous studies have shown cerebellar alterations in CHD.[67]

The underlying pathophysiology for adverse cerebral development in CHD is indeed multifactorial; however, neonatal environmental factors play a key role in this etiology.[68,69] Central to this is the link between reduced fetal cerebral oxygen delivery and impaired brain development in complex CHD.[69] The lack of oxygen delivery and adverse impact on brain growth is demonstrated in a CHD animal model where cerebral hypoxia reduces proliferation and neurogenesis in the subventricular zone in the postnatal brain resulting in an impaired cortical growth.[70] Also, insults associated with cardiopulmonary bypass cause WM vulnerability in animal CHD models.[71] Parallel to this, subcortical morphological reductions are associated with an altered metabolism in cerebral WM in both preterm and term infants with CHDs.[72] Overall, indices of a cerebral vulnerability to environmental factors in the perinatal period are present and may be highly relevant in the understanding of the adverse long-term brain development in CHD.

Another relevant aspect of the etiology is a potential genetic contribution. Homsy et al. reported that patients with both CHD and neurodevelopmental disabilities had a higher prevalence of de novo mutations, particularly in genes expressed in the developing heart and brain.[73] Their findings are consistent with those of Ji et al., who showed that neurodevelopmental disability in patients with CHDs may be attributable to genes altering both cardiac patterning and the neural connectivity.[74] As neurodevelopmental disabilities are common in our cohort of simple CHDs, a genetic contribution may therefore also be relevant to the etiology of altered cerebral microstructural tissue composition in this population.

DKI and Clinical Utility

Normal values for MKT in brain tissue have not yet been fully established and unfortunately these values seem to depend on the MRI scanner, sequence, and post hoc analyses used when obtaining the data. Fortunately, the different types of brain tissue demonstrates a consistent order in MKT value, meaning that WM has a higher MKT than GM and subcortical GM has a higher MKT than cortical GM because of penetrating WM fibers.[75] In an approach to establish reference values in healthy individuals, Maiter et al. demonstrated a cortical GM MKT of 0.82, subcortical GM MKT of 1.17, and WM MKT of 1.19 in healthy volunteers. Our MKT values showed the same consistent order with increasing MKT from cortical to subcortical GM; however, we found lower subcortical GM MKT values ranging from 0.7 to 1.2 depending on the nucleus. In support of our subcortical findings 2 other studies from our research institution demonstrated similar subcortical MKT values despite using another MRI scanner and sequence: Næss-Schmidt et al. demonstrated a thalamus MKT of 0.72 (in our study 0.83) and a MKT in hippocampus of 0.60 (in our study 0.71) in a control group,[76] and Nygaard et al. found a thalamus MKT of 0.63 and hippocampus MKT of 0.56 in patients with multiple sclerosis.[77] It appears that the order of the presented GM MKT values in our study is consistent with that reported by others, yet a quantitative comparison of MKT values across studies is not possible, and therefore, neither normative values nor change in MKT have a clinical significance at present. In addition, an age-related effect on non-Gaussian diffusion must also be taken into count when interpreting brain MKT values.[16] Consequently, MKT is considered a research tool, but with appropriate development and refinement it may evolve into clinical utility but much more experience is needed for interpretation of the results in a clinical scenario.

Limitations

Our study has inherent limitations. First, the cross-sectional design entails the risk of cohort selection bias with a possible overestimation of cerebral alterations. Second, the surgical treatments were performed over a period of ≈10 years and may suffer from variations in surgical techniques and perioperative care. Moreover, current guidelines recommend an earlier age at defect closure than in the 1990s, wherefore our findings may not mirror brain development in ASDs and VSDs operated today. Conversely, the cerebral alterations may

Table 4. Associations Between Neurodevelopmental Outcomes and Mean Values Within Clusters With Altered Cortical Diffusional Kurtosis Imaging Parameters for Participants With Congenital Heart Defect

	R^2	B	SE B	t	*P* value
Atrial septal defect					
Social recognition* versus MKT cluster in parietal lobe	0.43	0.0011	0.0004	2.44	0.021
Intelligence† versus MKT cluster at pericalcarine gyrus	0.50	0.0003	0.0002	2.16	0.047
Ventricular septal defect					
Verbal learning and memory‡ versus mean diffusivity cluster in parieto-occipital fissure	0.25	0.0014	0.0005	2.71	0.012
Congenital heart defect					
Intelligence† versus MKT cluster at pericalcarine gyrus	0.50	0.0003	0.0001	3.25	0.002

Data are presented as R^2, B±SE, t, and *P* value from a multivariable linear regression model adjusted for sex and age. None of the associations remained significant after false discovery rate adjustment at $q<0.05$. MKT indicates mean kurtosis tensor.

*Reading the Mind in the Eyes Test.

†Wechsler Adult Intelligence Scale Version IV, processing speed index.

‡Rey Auditory Verbal Learning Test, Delayed Recall Test.

be established during intrauterine brain development due to environmental factors as in complex CHD and may therefore continue to be a problem for today's patients. Third, the study lacks genetic testing. Excluding known associated genetic disorders, such as Trisomy 21 (Down's syndrome) and 22q11.2 deletion syndrome (DiGeorge syndrome), may not be sufficient because other genetic factors associated with CHD, such as de novo mutations[73] or epigenetic insults, may be relevant determinants in explaining our findings. Finally, a large variation in DKI parameter values across the cortical GM was observed in the groups with ASDs and VSDs compared with controls. One may speculate whether this variation highlights an unknown precision of using DKI to examine this study population. However, the large variation in DKI values was not present in the control group and in a test-retest study using a similar MRI scanner, the MKT coefficient varied only 2.9% in WM.[78] The DKI variation may very well define the composition of GM microstructure in a subgroup rather than being a general descriptive factor for the cohort with CHDs and could potentially conceal a higher level of GM microstructural abnormalities occurring in the affected patients with simple CHDs.

CONCLUSIONS

We identified altered microstructural tissue composition in the cerebral cortex and subcortical structures among adults, who in childhood underwent surgical closure of an ASD or VSD, when compared with healthy controls matched on age, sex, and educational attainment. Changes in microstructural composition were present in the left and right hemisphere cortex with distinct cluster-specific alterations located in the right occipital and parietal lobes. Subcortical microstructural changes were

Table 5. Associations Between Neurodevelopmental Outcomes and Subcortical Structures With Differences in Diffusional Kurtosis Imaging Parameters for Participants With Atrial Septal Defect

	R^2	B	SE B	t	*P* value
Processing speed* versus left caudate nucleus MKT	0.32	0.0005	0.0002	2.26	0.032
Verbal learning and memory† versus left caudate nucleus MKT	0.30	−0.0008	0.0004	−2.07	0.047
Executive function‡ versus left fornix MKT	0.38	0.0112	0.0031	3.57	0.001§
Executive function‡ versus left fornix MD	0.35	−0.0434	0.0122	−3.57	0.001*
Executive function‡ versus right thalamus MD	0.28	−0.0058	0.0019	−3.00	0.005

Data are presented as R^2, B±SE, t, and *P*-value from a multivariable linear regression model adjusted for sex and age. MD indicates mean diffusivity; and MKT, mean kurtosis tensor.

*Wechsler Adult Intelligence Scale Version IV.

†Rey Auditory Verbal Learning Test, Delayed Recall Test.

‡Delis-Kaplan Executive Function System, Verbal Fluency Test.

§false discovery rate $q<0.05$.

mainly located in the right hemisphere. The variations in cerebral microstructural tissue composition were associated with neuropsychological performance in both the groups with ASDs and VSDs. These findings suggest the presence of a compromised long-term cerebral microstructural tissue composition that may mirror a divergence in early neurodevelopment.

ARTICLE INFORMATION

Received January 16, 2021; accepted March 2, 2022.

Affiliations

Department of Cardiothoracic & Vascular Surgery (B.A., C.S., J.H.) and Neuroradiology Research Unit, Department of Radiology (L.O.), Aarhus University Hospital, Denmark; Center of Functionally Integrative Neuroscience (L.Ø., S.F.E.) and Department of Clinical Medicine (B.A., L.E., J.H., L.Ø., S.F.E., V.E.H.), Aarhus University, Denmark; Hammel Neurorehabilitation Centre and University Research Clinic, Denmark (L.E.); and Department of Cardiothoracic Surgery, Rigshospitalet and Institute of Clinical Medicine, University of Copenhagen, Denmark (V.E.H.).

Sources of Funding

This study was supported by Aarhus University, Aase & Ejnar Danielsens Foundation, The Danish Medical Association, A.P. Møller Foundation for the Advancement of Medical Science, Helga and Peter Korning Foundation, and the Health Research Fund of Central Denmark Region. Vibeke Elisabeth Hjortdal was financed on a grant from Novo Nordisk Foundation project no: NNFSA170030576.

Disclosures

None.

REFERENCES

1. Bellinger DC, Wypij D, Kuban KCK, Rappaport LA, Hickey PR, Wernovsky G, Jonas RA, Newburger JW. Developmental and neurological status of children at 4 years of age after heart surgery with hypothermic circulatory arrest or low-flow cardiopulmonary bypass. *Circulation*. 1999;100:526–532. doi: 10.1161/01.CIR.100.5.526
2. Gaynor JW, Stopp C, Wypij D, Andropoulos DB, Atallah J, Atz AM, Beca J, Donofrio MT, Duncan K, Ghanayem NS, et al. Neurodevelopmental outcomes after cardiac surgery in infancy. *Pediatrics*. 2015;135:816–825. doi: 10.1542/peds.2014-3825
3. Bellinger DC, Wypij D, Rivkin MJ, Demaso DR, Robertson RL, Dunbar-Masterson C, Rappaport LA, Wernovsky G, Jonas RA, Newburger JW. Adolescents with d-transposition of the great arteries corrected with the arterial switch procedure: neuropsychological assessment and structural brain imaging. *Circulation*. 2011;124:1361–1369. doi: 10.1161/CIRCULATIONAHA.111.026963
4. Miller SP, McQuillen PS, Hamrick S, Xu D, Glidden DV, Charlton N, Karl T, Azakie A, Ferriero DM, Barkovich AJ, et al. Abnormal brain development in newborns with congenital heart disease. *N Engl J Med*. 2007;357:1928–1938. doi: 10.1056/NEJMoa067393
5. Licht DJ, Shera DM, Clancy RR, Wernovsky G, Montenegro LM, Nicolson SC, Zimmerman RA, Spray TL, Gaynor JW, Vossough A. Brain maturation is delayed in infants with complex congenital heart defects. *J Thorac Cardiovasc Surg*. 2009;137:529–537. doi: 10.1016/j.jtcvs.2008.10.025
6. Limperopoulos C, Tworetzky W, McElhinney DB, Newburger JW, Brown DW, Robertson RL, Guizard N, McGrath E, Geva J, Annese D, et al. Brain volume and metabolism in fetuses with congenital heart disease: evaluation with quantitative magnetic resonance imaging and spectroscopy. *Circulation*. 2010;121:26–33. doi: 10.1161/CIRCULATIONAHA.109.865568
7. Ortinau C, Inder T, Lambeth J, Wallendorf M, Finucane K, Beca J. Congenital heart disease affects cerebral size but not brain growth. *Pediatr Cardiol*. 2012;33:1138–1146. doi: 10.1007/s00246-012-0269-9
8. Von Rhein M, Buchmann A, Hagmann C, Dave H, Bernet V, Scheer I, Knirsch W, Latal B, Heart and Brain Research Group. Severe congenital heart defects are associated with global reduction of neonatal brain volumes. *J Pediatr*. 2015;167:1259–1263.
9. Von Rhein M, Buchmann A, Hagmann C, Huber R, Klaver P, Knirsch W, Latal B. Brain volumes predict neurodevelopment in adolescents after surgery for congenital heart disease. *Brain*. 2014;137:268–276. doi: 10.1093/brain/awt322
10. Rollins CK, Watson CG, Asaro LA, Wypij D, Vajapeyam S, Bellinger DC, Demaso DR, Robertson RL, Newburger JW, Rivkin MJ. White matter microstructure and cognition in adolescents with congenital heart disease. *J Pediatr*. 2014;165:936–944.e2.
11. Brewster RC, King TZ, Burns TG, Drossner DM, Mahle WT. White matter integrity dissociates verbal memory and auditory attention span in emerging adults with congenital heart disease. *J Int Neuropsychol Soc*. 2015;21:22–33. doi: 10.1017/S135561771400109X
12. Rivkin MJ, Watson CG, Scoppettuolo LA, Wypij D, Vajapeyam S, Bellinger DC, Demaso DR, Robertson RL, Newburger JW. Adolescents with D-transposition of the great arteries repaired in early infancy demonstrate reduced white matter microstructure associated with clinical risk factors. *J Thorac Cardiovasc Surg*. 2013;146:543–549. doi: 10.1016/j.jtcvs.2012.12.006
13. Zaidi AH, Newburger JW, Wypij D, Stopp C, Watson CG, Friedman KG, Rivkin MJ, Rollins CK. Ascending aorta size at birth predicts white matter microstructure in adolescents who underwent Fontan palliation. *J Am Heart Assoc*. 2018;7:e010395. doi: 10.1161/JAHA.118.010395
14. Watson CG, Stopp C, Wypij D, Bellinger DC, Newburger JW, Rivkin MJ. Altered white matter microstructure correlates with IQ and processing speed in children and adolescents post-Fontan. *J Pediatr*. 2018;200:140–149.e4. doi: 10.1016/j.jpeds.2018.04.022
15. Panigrahy A, Schmithorst VJ, Wisnowski JL, Watson CG, Bellinger DC, Newburger JW, Rivkin MJ. Relationship of white matter network topology and cognitive outcome in adolescents with D-transposition of the great arteries. *NeuroImage Clin*. 2015;7:438–448. doi: 10.1016/j.nicl.2015.01.013
16. Falangola MF, Jensen JH, Babb JS, Hu C, Castellanos FX, Di Martino A, Ferris SH, Helpern JA. Age-related non-Gaussian diffusion patterns in the prefrontal brain. *J Magn Reson Imaging*. 2008;28:1345–1350. doi: 10.1002/jmri.21604
17. Helpern JA, Adisetiyo V, Falangola MF, Hu C, Di Martino A, Williams K, Castellanos FX, Jensen JH. Preliminary evidence of altered gray and white matter microstructural development in the frontal lobe of adolescents with attention-deficit hyperactivity disorder: a diffusional kurtosis imaging study. *J Magn Reson Imaging*. 2011;33:17–23. doi: 10.1002/jmri.22397
18. Steven AJ, Zhuo J, Melhem ER. Diffusion kurtosis imaging: an emerging technique for evaluating the microstructural environment of the brain. *Am J Roentgenol*. 2014;202:W26–W33 doi: 10.2214/AJR.13.11365
19. Jensen J, Helpern J. Quantifying non-Gaussian water diffusion by means of pulsed-field-gradient MRI. *Proc Int Soc Magn Reson Med*. 2003;859:2154.
20. Jensen JH, Helpern JA, Ramani A, Lu H, Kaczynski K. Diffusional kurtosis imaging: the quantification of non-Gaussian water diffusion by means of magnetic resonance imaging. *Magn Reson Med*. 2005;53:1432–1440. doi: 10.1002/mrm.20508
21. Lu H, Jensen JH, Ramani A, Helpern JA. Three-dimensional characterization of non-Gaussian water diffusion in humans using diffusion kurtosis imaging. *NMR Biomed*. 2006;19:236–247. doi: 10.1002/nbm.1020
22. Cheung MM, Hui ES, Chan KC, Helpern JA, Qi L, Wu EX. Does diffusion kurtosis imaging lead to better neural tissue characterization? A rodent brain maturation study.*NeuroImage*. 2009;45:386–392. doi: 10.1016/j.neuroimage.2008.12.018
23. Asschenfeldt B, Evald L, Heiberg J, Salvig C, Østergaard L, Dalby RB, Eskildsen SF, Hjortdal VE. Neuropsychological status and structural brain imaging in adults with simple congenital heart defects closed in childhood. *J Am Heart Assoc*. 2020;9:e015843. doi: 10.1161/JAHA.120.015843
24. Marques JP, Kober T, Krueger G, van der Zwaag W, Van de Moortele PF, Gruetter R. MP2RAGE, a self bias-field corrected sequence for improved segmentation and T1-mapping at high field. *NeuroImage*. 2010;49:1271–1281. doi: 10.1016/j.neuroimage.2009.10.002
25. Aubert-Broche B, Fonov VS, García-Lorenzo D, Mouiha A, Guizard N, Coupé P, Eskildsen SF, Collins DL. A new method for structural volume analysis of longitudinal brain MRI data and its application in studying the growth trajectories of anatomical brain structures in childhood. *NeuroImage*. 2013;82:393–402. doi: 10.1016/j.neuroimage.2013.05.065
26. Coupé P, Manjón JV, Fonov V, Pruessner J, Robles M, Collins DL. Patch-based segmentation using expert priors: application to hippocampus

and ventricle segmentation. *NeuroImage*. 2011;54:940–954. doi: 10.1016/j.neuroimage.2010.09.018
27. Eskildsen SF, Østergaard LR. Active surface approach for extraction of the human cerebral cortex from MRI. In: Larsen R, Nielsen M, Sporring J, eds. *Lecture Notes in Computer Science (including subseries Lecture Notes in Artificial Intelligence and Lecture Notes in Bioinformatics)*. Springer, Berlin Heidelberg: Berlin, Heidelberg; 2006:823–830.
28. Veraart J, Novikov DS, Christiaens D, Ades-aron B, Sijbers J, Fieremans E. Denoising of diffusion MRI using random matrix theory. *NeuroImage*. 2016;142:394–406. doi: 10.1016/j.neuroimage.2016.08.016
29. Kellner E, Dhital B, Kiselev VG, Reisert M. Gibbs-ringing artifact removal based on local subvoxel-shifts. *Magn Reson Med*. 2016;76:1574–1581. doi: 10.1002/mrm.26054
30. Andersson JLR, Sotiropoulos SN. An integrated approach to correction for off-resonance effects and subject movement in diffusion MR imaging. *NeuroImage*. 2016;125:1063–1078. doi: 10.1016/j.neuroimage.2015.10.019
31. Hansen B, Lund TE, Sangill R, Stubbe E, Finsterbusch J, Jespersen SN. Experimental considerations for fast kurtosis imaging. *Magn Reson Med*. 2016;76:1455–1468. doi: 10.1002/mrm.26055
32. Collignon A, Maes F, Delaere D, Vandermeulen D, Suetens P, Marchal G. Automated multi-modality image registration based on information theory. *Inf Process Med Imaging*. 1995;3:263–274.
33. Eskildsen SF, Østergaard LR. Evaluation of five algorithms for mapping brain cortical surfaces. In: *Proceedings - 21st Brazilian Symposium on Computer Graphics and Image Processing, SIBGRAPI 2008*. IEEE Computer Society Press; 2008:137–144.
34. Fonov V, Evans AC, Botteron K, Almli CR, McKinstry RC, Collins DL. Unbiased average age-appropriate atlases for pediatric studies. *NeuroImage*. 2011;54:313–327. doi: 10.1016/j.neuroimage.2010.07.033
35. Braaten EB. Wechsler adult intelligence scale. *SAGE Encycl Intellect Dev Disord*. 2018. doi: 10.4135/9781483392271.n535
36. Sue Baron I. Delis-Kaplan executive function system. *Child Neuropsychol*. 2004;10:147–152. doi: 10.1080/09297040490911140
37. Rey A. L'examen psychologique dans les cas d'encéphalopathie traumatique. *Arch Psychol (Geneve)*. 1941;28:215–285.
38. Osterreith PA. Le test de copie d'une figure complex: contribution à l'étude de la perception et de la memoir. *Arch Psychol (Geneve)*. 1944;286–356.
39. Meyers JE, Meyers KR. *Rey Complex Figure Test and Recognition Trial: Professional Manual*. Odessa, FL: Psychological Assessment Resources, Inc; 1995.
40. Rey A. Mémorisation d'une série de 15 mots en 5 répetitions. In: *L'examen clinique en psycologie*. Paris: Press Univ des France; 1958.
41. Baron-Cohen S, Wheelwright S, Hill J, Raste Y, Plumb I. The, "Reading the Mind in the Eyes" Test revised version: a study with normal adults, and adults with Asperger syndrome or high-functioning autism. *J Child Psychol Psychiatry Allied Discip*. 2001;42:241–251. doi: 10.1111/1469-7610.00715
42. Benjamini Y, Hochberg Y. Controlling the false discovery rate: a practical and powerful approach to multiple testing. *J R Stat Soc Ser B*. 1995;57:289–300. doi: 10.1111/j.2517-6161.1995.tb02031.x
43. Worsley K, Taylor J, Carbonell F, Chung M, Duerden E, Bernhardt B, Lyttelton O, Boucher M, Evans A. SurfStat: a Matlab toolbox for the statistical analysis of univariate and multivariate surface and volumetric data using linear mixed effects models and random field theory. *NeuroImage*. 2009;47:S102. doi: 10.1016/S1053-8119(09)70882-1
44. Worsley KJ, Marrett S, Neelin P, Vandal AC, Friston KJ, Evans AC. A unified statistical approach for determining significant signals in images of cerebral activation. *Hum Brain Mapp*. 1996;4:58–73. doi: 10.1002/(SICI)1097-0193(1996)4:1<58:AID-HBM4>3.0.CO;2-O
45. Bester M, Jensen JH, Babb JS, Tabesh A, Miles L, Herbert J, Grossman RI, Inglese M. Non-Gaussian diffusion MRI of gray matter is associated with cognitive impairment in multiple sclerosis. *Mult Scler*. 2015;21:935–944. doi: 10.1177/1352458514556295
46. Wu EX, Cheung MM. MR diffusion kurtosis imaging for neural tissue characterization. *NMR Biomed*. 2010;23:836–848.
47. Irie R, Kamagata K, Kerever A, Ueda R, Yokosawa S, Otake Y, Ochi H, Yoshizawa H, Hayashi A, Tagawa K, et al. The relationship between neurite density measured with confocal microscopy in a cleared mouse brain and metrics obtained from diffusion tensor and diffusion kurtosis imaging. *Magn Reson Med Sci*. 2018;17:138–144. doi: 10.2463/mrms.mp.2017-0031
48. Adisetiyo V, Tabesh A, Di Martino A, Falangola MF, Castellanos FX, Jensen JH, Helpern JA. Attention-deficit/hyperactivity disorder without comorbidity is associated with distinct atypical patterns of cerebral microstructural development. *Hum Brain Mapp*. 2014;35:2148–2162. doi: 10.1002/hbm.22317
49. Guan J, Ma X, Geng Y, Qi D, Shen Y, Shen Z, Chen Y, Wu E, Wu R. Diffusion kurtosis imaging for detection of early brain changes in Parkinson's disease. *Front Neurol*. 2019;10:1285. doi: 10.3389/fneur.2019.01285
50. McKenna FF, Miles L, Babb JS, Goff DC, Lazar M. Diffusion kurtosis imaging of gray matter in schizophrenia. *Cortex*. 2019;121:201–224. doi: 10.1016/j.cortex.2019.08.013
51. Blockx I, Verhoye M, Van Audekerke J, Bergwerf I, Kane JX, Delgado y Palacios R, Veraart J, Jeurissen B, Raber K, von Hörsten S, et al. Identification and characterization of Huntington related pathology: an in vivo DKI imaging study. *NeuroImage*. 2012;63:653–662. doi: 10.1016/j.neuroimage.2012.06.032
52. Vanhoutte G, Pereson S, Delgado y Palacios R, Guns P-J, Asselbergh B, Veraart J, Sijbers J, Verhoye M, Van Broeckhoven C, Van der Linden A. Diffusion kurtosis imaging to detect amyloidosis in an APP/PS1 mouse model for Alzheimer's disease. *Magn Reson Med*. 2013;69:1115–1121. doi: 10.1002/mrm.24680
53. Zhuo J, Xu S, Proctor JL, Mullins RJ, Simon JZ, Fiskum G, Gullapalli RP. Diffusion kurtosis as an in vivo imaging marker for reactive astrogliosis in traumatic brain injury. *NeuroImage*. 2012;59:467–477. doi: 10.1016/j.neuroimage.2011.07.050
54. McMackin D, Cockburn J, Anslow P, Gaffan D. Correlation of fornix damage with memory impairment in six cases of colloid cyst removal. *Acta Neurochir (Wien)*. 1995;135:12–18. doi: 10.1007/BF02307408
55. Mielke MM, Okonkwo OC, Oishi K, Mori S, Tighe S, Miller MI, Ceritoglu C, Brown T, Albert M, Lyketsos CG. Fornix integrity and hippocampal volume predict memory decline and progression to Alzheimer's disease. *Alzheimer's Dement*. 2012;8:105–113. doi: 10.1016/j.jalz.2011.05.2416
56. Hooper MW, Vogel FS. The limbic system in Alzheimer's disease. A Neuropathologic Investigation. *Am J Pathol*. 1976;85:1–20.
57. Bagge CN, Henderson VW, Laursen HB, Adelborg K, Olsen M, Madsen NL. Risk of dementia in adults with congenital heart disease: population-based cohort study. *Circulation*. 2018;137:1912–1920. doi: 10.1161/CIRCULATIONAHA.117.029686
58. Watson CG, Asaro LA, Wypij D, Robertson RL, Newburger JW, Rivkin MJ. Altered gray matter in adolescents with D-transposition of the great arteries portions of the study were presented as a poster at the meeting of the child neurology society, Huntington beach, CA, October 31-November 2, 2012. *J Pediatr*. 2016;169:36–43.e1.
59. Matthiesen NB, Østergaard JR, Hjortdal VE, Henriksen TB. Congenital heart defects and the risk of spontaneous preterm birth. *J Pediatr*. 2021;229:168–174.e5. doi: 10.1016/j.jpeds.2020.09.059
60. Matthiesen NB, Henriksen TB, Gaynor JW, Agergaard P, Bach CC, Hjortdal VE, Østergaard JR. Congenital heart defects and indices of fetal cerebral growth in a nationwide cohort of 924 422 liveborn infants. *Circulation*. 2016;133:566–575. doi: 10.1161/CIRCULATIONAHA.115.019089
61. Matthiesen NB, Henriksen TB, Agergaard P, Gaynor JW, Bach CC, Hjortdal VE, Østergaard JR. Congenital heart defects and indices of placental and fetal growth in a nationwide study of 924 422 liveborn infants. *Circulation*. 2016;134:1546–1556.
62. Latal B, Patel P, Liamlahi R, Knirsch W, O'Gorman Tuura R, Von Rhein M. Hippocampal volume reduction is associated with intellectual functions in adolescents with congenital heart disease. *Pediatr Res*. 2016;80:531–537. doi: 10.1038/pr.2016.122
63. Marelli A, Miller SP, Marino BS, Jefferson AL, Newburger JW. Brain in congenital heart disease across the lifespan: the cumulative burden of injury. *Circulation*. 2016;133:1951–1962. doi: 10.1161/CIRCULATIONAHA.115.019881
64. Von Rhein M, Scheer I, Loenneker T, Huber R, Knirsch W, Latal B. Structural brain lesions in adolescents with congenital heart disease. *J Pediatr*. 2011;158:984–989. doi: 10.1016/j.jpeds.2010.11.040
65. Heinrichs AKM, Holschen A, Krings T, Messmer BJ, Schnitker R, Minkenberg R, Hövels-Gürich HH. Neurologic and psycho-intellectual outcome related to structural brain imaging in adolescents and young adults after neonatal arterial switch operation for transposition of the great arteries. *J Thorac Cardiovasc Surg*. 2014;148:2190–2199. doi: 10.1016/j.jtcvs.2013.10.087
66. Bellinger DC, Watson CG, Rivkin MJ, Robertson RL, Roberts AE, Stopp C, Dunbar-Masterson C, Bernson D, DeMaso DR, Wypij D, et al. Neuropsychological status and structural brain imaging in adolescents with single ventricle who underwent the Fontan procedure. *J Am Heart Assoc*. 2015;4:e002302. doi: 10.1161/JAHA.115.002302

67. Olshaker H, Ber R, Hoffman D, Derazne E, Achiron R, Katorza E. Volumetric brain MRI study in fetuses with congenital heart disease. *Am J Neuroradiol*. 2018;39:1164–1169. doi: 10.3174/ajnr.A5628
68. Lauridsen MH, Uldbjerg N, Henriksen TB, Petersen OB, Stausbøl-Grøn B, Matthiesen NB, Peters DA, Ringgaard S, Hjortdal VE. Cerebral oxygenation measurements by magnetic resonance imaging in fetuses with and without heart defects. *Circ Cardiovasc Imaging*. 2017;10:e006459. doi: 10.1161/CIRCIMAGING.117.006459
69. Sun L, Macgowan CK, Sled JG, Yoo S-J, Manlhiot C, Porayette P, Grosse-Wortmann L, Jaeggi E, McCrindle BW, Kingdom J, et al. Reduced fetal cerebral oxygen consumption is associated with smaller brain size in fetuses with congenital heart disease. *Circulation*. 2015;131:1313–1323. doi: 10.1161/CIRCULATIONAHA.114.013051
70. Morton PD, Korotcova L, Lewis BK, Bhuvanendran S, Ramachandra SD, Zurakowski D, Zhang J, Mori S, Frank JA, Jonas RA, et al. Abnormal neurogenesis and cortical growth in congenital heart disease. *Sci Transl Med*. 2017;9. doi: 10.1126/scitranslmed.aah7029
71. Stinnett GR, Lin S, Korotcov AV, Korotcova L, Morton PD, Ramachandra SD, Pham A, Kumar S, Agematsu K, Zurakowski D, et al. Microstructural alterations and oligodendrocyte dysmaturation in white matter after cardiopulmonary bypass in a juvenile porcine model. *J Am Heart Assoc*. 2017;6. doi: 10.1161/JAHA.117.005997
72. Gertsvolf N, Votava-Smith JK, Ceschin R, del Castillo S, Lee V, Lai HA, Bluml S, Paquette L, Panigrahy A. Association between subcortical morphology and cerebral white matter energy metabolism in neonates with congenital heart disease. *Sci Rep*. 2018;8:14057. doi: 10.1038/s41598-018-32288-3
73. Homsy J, Zaidi S, Shen Y, Ware JS, Samocha KE, Karczewski KJ, DePalma SR, McKean D, Wakimoto H, Gorham J, et al. De novo mutations in congenital heart disease with neurodevelopmental and other congenital anomalies. *Science*. 2015;350:1262–1266. doi: 10.1126/science.aac9396
74. Ji W, Ferdman D, Copel J, Scheinost D, Shabanova V, Brueckner M, Khokha MK, Ment LR. De novo damaging variants associated with congenital heart diseases contribute to the connectome. *Sci Rep*. 2020;10. doi: 10.1038/s41598-020-63928-2
75. Maiter A, Riemer F, Allinson K, Zaccagna F, Crispin-Ortuzar M, Gehrung M, McLean MA, Priest AN, Grist J, Matys T, et al. Investigating the relationship between diffusion kurtosis tensor imaging (DKTI) and histology within the normal human brain. *Sci Rep*. 2021;11:8857. doi: 10.1038/s41598-021-87857-w
76. Næss-Schmidt ET, Blicher JU, Eskildsen SF, Tietze A, Hansen B, Stubbs PW, Jespersen S, Østergaard L, Nielsen JF. Microstructural changes in the thalamus after mild traumatic brain injury: a longitudinal diffusion and mean kurtosis tensor MRI study. *Brain Inj*. 2017;31:230–236. doi: 10.1080/02699052.2016.1229034
77. Nygaard MKE, Langeskov-Christensen M, Dalgas U, Eskildsen SF. Cortical diffusion kurtosis imaging and thalamic volume are associated with cognitive and walking performance in relapsing–remitting multiple sclerosis. *J Neurol*. 2021;268:3861–3870. doi: 10.1007/s00415-021-10543-4
78. Shahim P, Holleran L, Kim JH, Brody DL. Test-retest reliability of high spatial resolution diffusion tensor and diffusion kurtosis imaging. *Sci Rep*. 2017;7:11141. doi: 10.1038/s41598-017-11747-3